

Bitte beachten Sie, dass angeführte Nichtpatentliteratur (wie z. B. wissenschaftliche oder technische Dokumente) je nach geltendem Recht dem Urheberrechtsschutz und/oder anderen Schutzarten für schriftliche Werke unterliegen könnte. Die Vervielfältigung urheberrechtlich geschützter Texte, ihre Verwendung in anderen elektronischen oder gedruckten Publikationen und ihre Weitergabe an Dritte ist ohne ausdrückliche Zustimmung des Rechtsinhabers nicht gestattet.

Veuillez noter que les ouvrages de la littérature non-brevets qui sont cités, par exemple les documents scientifiques ou techniques, etc., peuvent être protégés par des droits d'auteur et/ou toute autre protection des écrits prévue par les législations applicables. Les textes ainsi protégés ne peuvent être reproduits ni utilisés dans d'autres publications électroniques ou imprimées, ni rediffusés sans l'autorisation expresse du titulaire du droit d'auteur.

Please be aware that cited works of non-patent literature such as scientific or technical documents or the like may be subject to copyright protection and/or any other protection of written works as appropriate based on applicable laws. Copyrighted texts may not be copied or used in other electronic or printed publications or re-distributed without the express permission of the copyright holder.

# Application of particle image velocimetry to large-scale transonic wind tunnels

C.E. TOWERS, P.J. BRYANSTON-CROSS, T.R. JUDGE

Velocity measurements have been made in a large-scale transonic wind tunnel using particle image velocimetry. Diffraction-limited optics have been used to image seeding particles at up to 2.5 m from the flow. A practical system to record the data has been constructed such that the camera can be remotely focused on the plane of interest. Particle images were recorded onto 35 mm film. Results were obtained from Mach numbers 0.2 to 0.8, and automatically analysed to produce vector maps of the planar velocity field. It has also been shown that particle image velocimetry data can be successfully recorded onto a charged coupled device image sensor at transonic speeds. This approach eliminates the need for photographic processing and allows real time data acquisition in a digital form. The potential is then apparent for automatic, and near real-time processing, of particle image velocimetry data.

KEYWORDS: velocimetry, diffraction-limited optics, photography, particle imaging

## Introduction

Particle image velocimetry (PIV), has been established as a non-intrusive, quantitative diagnostic for the planar velocity field in a flow<sup>1-4</sup>. The technique requires that a sheet of light be projected through the flow. Seeding particles are introduced so that light scattered from the particles is imaged directly onto film or a CCD (charged coupled device) sensor. Conventional photographic imaging methods are used.

In the experiments described, two laser pulses are used to form a double exposure photograph of the particles. By measuring the distance between a pair of particle images, and given the pulse separation, the velocity of the particle can be determined.

In this paper, for the first time, the use of a near diffraction-limited optic is demonstrated as a means to obtain satisfactory particle images at optical stand-off distances of up to 2.5 m. PIV data was obtained on 35 mm Kodak TMAX film<sup>5</sup>, and from a CCD.

The diffraction-limited optic was connected to a Canon F-1 single lens reflex camera, (SLR). A CCD sensor was mounted in the viewfinder of the camera.

Directly digitized PIV data was obtained in real time from the CCD sensor and a frame-grabber, contained in a PC. This eliminated the wet processing required for the development of photographic film.

A system was constructed to focus the camera remotely on different planes of the flow during testing. The camera and imaging optic were mounted on a linear traverse. Images obtained in real time from the CCD sensor were used to control the camera position. Therefore, it was possible to focus on the particle images.

This type of imaging system allows PIV to be applied to a wide range of industrially relevant problems. Results are shown from a large scale transonic wind tunnel.

Until recently, work in this field has concentrated on water flows and low-speed air flows, with the particle data being recorded onto photographic film. In the last two years, the technique has been applied to transonic and supersonic flows<sup>6,7</sup>.

From the work by Melling<sup>8</sup>, and laser anemometry studies, it has been shown that sub-micron particles are required to seed supersonic flows. The particles then represent the motion of the fluid at any point. However, the Mie light scattering theory<sup>9</sup>, implies that the amount of light scattered by such particles

The authors are in the Department of Engineering, Warwick University, Coventry CV4 7AL UK.  
Received 3 May 1991. Revised 18 September 1991.

is low. It has been shown by Bryanston-Cross<sup>6</sup> that  $0.5\text{ }\mu\text{m}$  polystyrene microspheres provide an acceptable compromise to this problem.

The test facility used to perform the experiments was a  $2.44 \times 2.74\text{ m}$  cross-section, transonic wind tunnel, (TWT), at the Aircraft Research Association (ARA), Bedford, UK<sup>10</sup>. The transonic flow around a model aircraft wing was investigated. The experiment was performed non-intrusively, with seeding particles introduced ~ 9 m upstream of the working section.

The problem of adequately seeding the flow is discussed. The number of seeding particles per unit volume was low, approximately 300 particle pairs per  $35\text{ mm}$  negative. Consequently, the data was processed by digitizing with a flat bed scanner and then directly pairing individual particles.

## Application of PIV to transonic flows

### Laser system

In the experiments performed, a frequency doubled Nd:YAG laser was used to form the light sheet. The output of the laser was Q-switched to give a pulse duration of  $10\text{ ns}$  at a wavelength of  $532\text{ nm}$ . The system was capable of producing two Q-switched pulses with pulse separations in the range from  $50\text{ ns}$  to  $100\text{ }\mu\text{s}$  (see Ref. 6).

The laser was operated in open lase mode at a repetition rate of  $10\text{ Hz}$  for alignment purposes. This removes any uncertainty in the focal plane of the light sheet which is present when a HeNe laser is used in conjunction with a ruby laser<sup>11</sup>.

The wavelength of the laser is well suited to the spectral sensitivity of the film used, Kodak TMAX 3200. This film has a resolution of  $100\text{ lines mm}^{-1}$ , and an ASA rating of 3200.

### Seeding material used

A balance must be achieved between the size of the seeding particles and the light scattered by the particles. The most effective particles found were polystyrene microspheres. These particles have a high quantum efficiency and can be produced in a range of sizes, from  $0.3$  to  $2.7\text{ }\mu\text{m}$  (see Refs 12, 13). The chemical reaction to produce the polymer chains of styrene automatically gives a spherical shape and uniform size to the particles. This was examined using a scanning electron microscope, see Fig. 1.

A validation of the flow-following characteristics of the particles was performed at MIT, Cambridge, Massachusetts, USA<sup>6</sup>. A prediction of the flow velocity through a normal shock was made. The experimental results correlated well to the predicted velocities. The velocity in this case was Mach 3, and  $0.5\text{ }\mu\text{m}$  particles were used to seed the flow.

### Long distance imaging of seeding particles for transonic PIV

In previous work, a conventional macro lens was used to image the particles in the flow<sup>6,7</sup>, at an

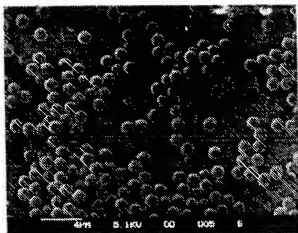


Fig. 1 Scanning electron microscope image of  $1.0\text{ }\mu\text{m}$  poly-styrene microspheres

object distance of  $120\text{ mm}$ . The resolution of the lens at this distance was found to be  $30\text{ }\mu\text{m}$  using a USAF test chart.

The lens contained simple geometric aberrations. This produced particle images larger than the predicted size from diffraction theory. Using sub-micron particles, the light collected is close to the fog level of the film. To increase the signal-to-noise ratio of the particle images, the use of a diffraction limited optic has been investigated.

A further problem was found from the use of a macro lens at large object distances, as a significant reduction in magnification is produced. This affects the particle separation in the image plane, and therefore the accuracy of the velocity measurements which can be made. To increase the distance between particle image pairs, and thereby the measurement accuracy, requires longer pulse separations.

The Nd:YAG laser used for the experiments, had a maximum pulse separation of  $100\text{ }\mu\text{s}$ . This limited the amount of magnification reduction in the image that could be accommodated.

A compromise must be found between the particle image spacing and the ability to make velocity measurements in a turbulent flow. The combination of turbulence, and long pulse separations, produces a greater probability of single particle images. In this case, it becomes difficult to correlate particle image pairs to obtain velocity measurements. Therefore, the application of long-range PIV to large-scale wind tunnels requires an optic with a small viewing angle and high spatial resolution.

### Diffraction-limited imaging

An initial investigation was performed using a Questar, QM1, long range microscope<sup>14</sup>. The QM1 is of Cassegrain design, with a clear aperture of  $88.9\text{ mm}$ . The optic was positioned  $1.3\text{ m}$  from a light sheet, and a plume of particles imaged directly from the outlet of a commercial seeder.

The images were recorded on TMAX 3200 film. A

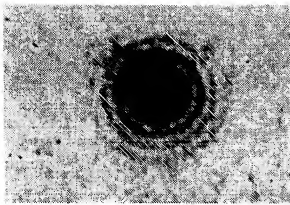


Fig. 2 Diffraction limited image of  $0.5 \mu\text{m}$  polystyrene microsphere

portion of the negative was enlarged onto a CCD sensor. A diffraction-limited image of a  $0.5 \mu\text{m}$  particle showing the Airy disc intensity pattern is seen in Fig 2. The spacing of the fringes agrees well with that expected from diffraction theory<sup>15,16</sup>.

An advantage of a diffraction-limited optic is the small image size observed at the film plane. As a consequence of this a lower energy laser pulse was required to obtain images with good signal-to-noise ratio. Reducing the pulse energy also reduces the scatter noise from any objects in the path of the laser sheet. Therefore, particles can be imaged closer to solid surfaces. In practice, an energy of  $5 \text{ mJ pulse}^{-1}$  was sufficient to produce images at a working distance of  $1.3 \text{ m}$  (compared to  $30 \text{ mJ pulse}^{-1}$  with a macro lens at a working distance of  $120 \text{ mm}$ ).

The magnification of the Questar was high, producing a field of view of only a few millimetres. When large flow volumes are to be examined the repositioning of the camera system, in order to map the required flow volume, is time consuming.

A K2 long range microscope with a magnification of  $0.3$  at a working distance of  $1.7 \text{ m}$  was evaluated<sup>17</sup>. This optic provided a field of view not dissimilar to the macro lens used at close range, and near diffraction limited performance. This optic has been used in the wind tunnel experiments and gives a good compromise between image quality, magnification, depth of field, and cost.

### Experimental arrangement for a large transonic wind tunnel

A diagram showing the cross-section of the transonic wind tunnel is shown in Fig. 3. The width of the working section is  $2.74 \text{ m}$ , by  $2.44 \text{ m}$  in height.

Experiments were performed on a  $1/20$  scale, half-span model of a civil aircraft with a turbine powered engine simulator, or TPS unit. The TPS is driven by compressed air and produces a central core jet surrounded by a by-pass jet. The exit pressures of the two flows model the real flow from a high-bypass turbofan engine. The flow is fully three-dimensional and highly turbulent. A range of free-stream flow speeds from  $0.2$  to  $0.8$  Mach number were examined.

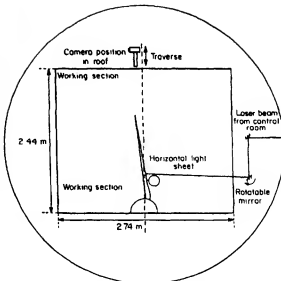


Fig. 3 Schematic drawing of the transonic wind tunnel at the Aircraft Research Association

Optical access is restricted to the tunnel walls and ceiling. The wind tunnel operates under sub-atmospheric conditions. To prevent de-tuning of the Nd:YAG laser during the test, the optical head of the laser was located in the control room of the tunnel,  $\sim 5.79 \text{ m}$  from the flow. The beam entered the wind tunnel through an armoured glass window, and was brought down to the correct height by a periscope of dielectric mirrors. A lens system formed a horizontal light sheet, which could be rotated vertically by a galvanometer to scan different planes. The camera system was mounted on a mechanical traverse, and placed in the tunnel roof at a distance of  $1.96 \text{ m}$  from the light sheet.

The transonic wind tunnel is a continuous running test facility. A problem encountered is the operational costs of the wind tunnel,  $\sim \$40\,000$  per day. The PIV data collection time for a  $36$  exposure film was approximately  $2 \text{ min}$ , from one plane position. This technique provides a fast accumulation of data compared with other laser diagnostic methods, such as LDA, which often operates at about one second per point.

### Seeding the transonic wind tunnel

An array of  $16$  nebulizers was used to seed the flow. A local seeding probe in the working section could not be used as this would cause a disturbance of the flow around the model. Therefore the seeding array was placed  $\sim 9 \text{ m}$  upstream of the model in the settling chamber of the wind tunnel, see Fig. 4. The array of nebulizers formed a  $1 \text{ m}$  diameter plume of seeded air in the settling chamber. The particles followed the flow through a contraction to form a plume,  $\sim 300 \text{ mm}$  in diameter, in the working section.

The seeding particle density was found to be  $\sim 3$  particle pairs  $\text{cm}^{-2}$  at a Mach number of  $0.2$ . This decreased to  $\sim 0.5$  particle pairs  $\text{cm}^{-2}$  at  $0.8$  Mach

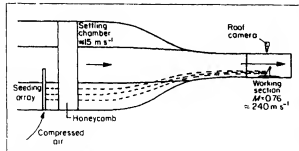


Fig. 4 Seeding arrangement for the transonic wind tunnel

number. This data was calculated from the PIV results.

The first experiment performed in the wind tunnel was to locate the seeding plume. A vertical light sheet was projected through the flow and a Cohu CCD camera<sup>19</sup>, placed in the tunnel floor, ~2 m down-stream of the civil aircraft model, in order to visualize the flow. An image showing the model wing and TPS unit, obtained from this camera position, is given in Fig. 5.

The seeding plume was found to be centred slightly above the TPS unit.

A laser-light sheet visualization was performed on the bypass flow from the TPS unit with this camera position. The core of the TPS unit is powered by unseeded compressed air, and only the bypass flow can be externally seeded. The visualization takes the form of a seeded hollow ring, representing the bypass, see Fig. 6. This image was produced at a Mach number of 0.6.

#### Camera focusing system

A Pulnix CCD sensor<sup>19</sup>, mounted in the viewfinder of the Canon F-1 (see Fig. 7), was linked to a frame-grabber inside a PC. The framestore was synchronized at 1 Hz to the pulse laser via an input/output card. The frame containing the pulsed PIV image was captured and held in the framestore, being refreshed at the next laser pulse. A monitor was linked to the output of the framestore, displaying the images during testing. This system was constructed for previous flow visualization work, see Ref. 20.

By displaying the particle images in real time the focusing of the camera was controlled. The focusing could be adjusted by traversing the camera system. This system had the potential to examine a volume of the flow by moving the light sheet and refocusing the camera on the new sheet position, without shutting down the wind tunnel.

A video recorder was also linked into the system to record the images from the CCD camera. Images of particle pairs were recorded on video-tape for flow speeds from 0.2 to 0.8 Mach number.

The size of the CCD sensor was  $\sim 7 \times 5 \text{ mm}$ . Hence, the field of view seen by the CCD camera was small compared with a 35 mm photographic negative. The pixel size of the CCD sensor is  $\sim 16 \mu\text{m}$ , compared to  $\sim 5 \mu\text{m}$  for the film used.

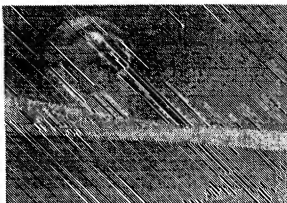


Fig. 5 Camera view of model wing and TPS unit

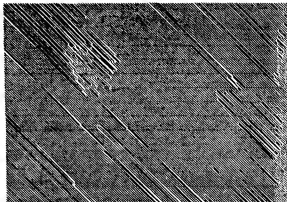


Fig. 6 Laser light sheet flow visualization of simulated gas turbine bypass flow

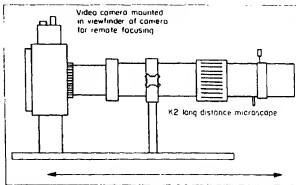


Fig. 7 Camera system incorporating K2 imaging lens and CCD camera

The two recording media (CCD and film) can be compared by forming a space bandwidth product (SBP). This is composed of two factors: the spatial resolution in lines  $\text{mm}^{-1}$ , and the size of the image sensor. The SBP for the 35 mm film used is approx 3500 (100 lines  $\text{mm}^{-1}$  resolution, and an image size of 35 mm). The SBP of the Pulnix CCD sensor was approx 200. Current developments in CCD technology has produced  $4096 \times 4096$  pixel sensors, with a SBP of  $\approx 2048$ . Therefore the SBP of CCD sensors

is approaching that of 35 mm film. With the development of larger CCD sensors which can operate at near video rates, the authors foresee CCD cameras and video rate frame-grabbers replacing photographic materials.

### Automatic analysis of sparse PIV data

The processing of the PIV data was performed automatically. The whole of the 35 mm negatives were enlarged to produce A4 size positive prints. A commercial flat bed scanner was used to digitize automatically the data. This device is used commercially in desk top publishing. The scanner has a spatial resolution of 300 dpi (dots per inch) and a grey scale range of 0 to 255. The digital image produced does not utilize the full resolution of the 35 mm negative. However, the whole field of view of the 35 mm camera is contained in the scanned digital image. In this work the scanner was also used to threshold the data, yielding a binary image.

A spatial domain algorithm was used to identify particle pairs automatically and calculate particle velocities. It was not practical to use frequency domain analysis methods<sup>3</sup> as the particle data collected at higher Mach numbers was sparse. A description of the algorithm is to be published in a separate paper<sup>21</sup>.

### Results and discussion

PIV data was obtained from two laser sheet positions. The results presented in this paper show the flow in a horizontal plane, around the leading edge of the wing just above the TPS unit, see Fig. 8. PIV results were obtained for this sheet position at Mach numbers 0.2, 0.4, 0.6, 0.8, with pulse separations from 3–10  $\mu$ s.

A photograph showing the field of view of the camera in the wind tunnel roof is given in Fig. 9. Each square in the grid represents 1 cm in object space. The black object at the bottom of the picture is the leading edge of the wing.

Two example PIV photographs are shown in Fig. 10 and Fig. 11, with free stream velocities of 0.2 and 0.8 Mach number respectively. The flow is from right to

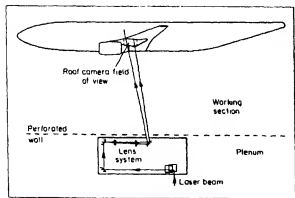


Fig. 8 Laser sheet position with field of view of camera

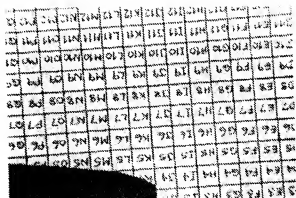


Fig. 9 Field of view of 35 mm SLR camera



Fig. 10 Particle image pairs for Mach number 0.2



Fig. 11 Particle image pairs for Mach number 0.8

left in the pictures. The solid bright region, represents light scattered from the wing surface caused by the light sheet impinging on the wing. It can be seen from the photographs that the seeding becomes less dense for the higher Mach numbers, i.e. the number of particles per unit volume decreases with increasing flow speed.

Similar results were obtained using the CCD sensor mounted in the view finder of the SLR camera, but over a smaller field of view. A typical image of

particle pairs is shown in Fig. 12. This image has been normalized and thresholded.

#### Processed data

Processed PIV data is presented in Figs 13 and 14, representing free-stream Mach numbers of 0.2 and 0.8 respectively. Each particle pair automatically detected by the algorithm is represented as an arrow. The size of the arrow indicates the magnitude of the velocity.

The region at the bottom of each plot represents the flare from the wing surface. The edge of the flare has been detected and drawn on the plots to provide a reference. Velocity measurements were made to 5 mm of the wing surface.

The three vectors shown at the extreme right hand side of Fig. 13 are erroneous and caused by noise points in the digitized and thresholded data. Similarly, in Fig. 14, the vectors in the top right hand corner, and the vector at the bottom right hand side, are incorrect.



Fig. 12 PIV image obtained with CCD camera

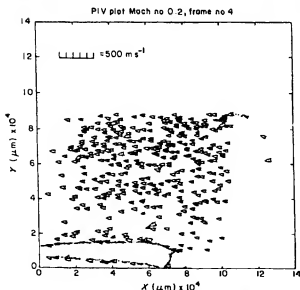


Fig. 13 Vector plot at free-stream speed of 0.2 Mach number

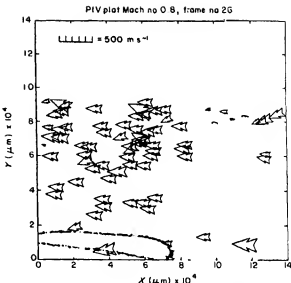


Fig. 14 Vector plot at free-stream speed of 0.8 Mach number

The automatic analysis software has been successful in extracting isolated particle pairs. In regions containing several particle pairs the algorithm disregards the information due to the ambiguities present in pairing the particle images. A manual analysis of the same data would extract more information as closely spaced particle pairs could be identified correctly.

The two main problems faced by the automatic analysis algorithm are described below.

- (i) Identifying the particle image data is dependent on the nature of the photographic development and the quality of the prints produced. The introduction of noise at any stage of the processing leads to marks on the prints which may then be detected as particle images.
- (ii) The correct detection of particles is conditional on the threshold level set in the scanner. Uneven energies in the two laser pulses emphasizes the problem of assigning the appropriate threshold level. This can result in a higher number of single particle images which cannot be paired.

The velocities furthest from the wing surface correlate well with the free-stream Mach numbers in each case. Further verification of the results was obtained by analysing flow conditions with the same free-stream Mach number, but different angles of incidence for the wing. This data showed the expected trends in direction changes around the leading edge of the wing. A more detailed comparison with the results from a computational fluid dynamics code is a topic of further work.

#### Accuracy of measurements

The main error source in the velocity measurements is caused by the separation of the particle images in the digitized data. For the 0.8 Mach number results,

the average particle separation was 55 pixels. The accuracy of the measurements is then 3.5%. This assumes that the particle separation can be measured to 2 pixels, i.e. 1 pixel uncertainty in determining the centre of each particle. Higher precision measurements were not made owing to the limited run time available.

Two other error sources have been considered.

- (i) In the experiments, a maximum of 5° deviation from normal viewing was present between the observation direction and the laser light sheet. The error is a function of the cosine of the angle.
- (ii) A high-resolution oscilloscope is required to define accurately the pulse separation from the laser.

These two error sources combined produce an error of 0.5% to the velocity measurements. Therefore the velocity measurements at 0.8 Mach number could be made to within 4%.

## Conclusions

The application of PIV to a large-scale transonic wind tunnel has been presented. A remote seeding rig successfully introduced seeding ~ 9 m upstream of the working section of the tunnel.

It has been demonstrated that a diffraction-limited optics allows the working range of PIV systems to be extended to several metres. Hence, a large range of industrial applications have now become possible. The use of diffraction-limited imaging has also been shown to reduce significantly the laser energy required to form satisfactory particle images.

PIV data has been recorded onto 35 mm film, and automatically analysed, to produce velocity vector maps of the flow. Velocity measurements at 0.8 Mach number were made to an accuracy of 4%. By increasing the pulse separation from the laser it should be possible to obtain measurements to 0.5%.

Particle images were also recorded directly onto a CCD sensor and digitized at video rates. From this result it is foreseen that CCD sensors will replace photographic materials for PIV. With the advent of large CCD sensors with video-rate read out times, a comparable spatial resolution to 35 mm film will be attainable.

A system has been constructed to focus the camera remotely on different planes of the flow during a single wind tunnel test. The potential is to examine a volume of the flow in a matter of minutes thereby reducing operating costs.

## Acknowledgements

The authors would like to thank the staff of the

Aircraft Research Association Ltd for their support during this work, and the DTI and SERC for funding the research under the LINK scheme programme.

## References

- 1 Pickering, C.J.D., Halliwell, N.A. Particle Image Velocimetry: A New Field Measurement Technique. Optical Measurement in Fluid Mechanics. Institute of Physics conference series. 1977 Adam Hilger, Bristol (1985)
- 2 Meynart, R. 'Equal velocity fringes in a Rayleigh-Benard flow by a speckle method'. *Appl Opt* 19 (9) (1980)
- 3 Adrian, R., Yao, C. 'Pulsed laser technique application to liquid and gaseous flows and the scattering power of seed materials'. *Appl Opt* 24 (1) (1985)
- 4 Trolinger, J.D. 'Laser Applications in Flow Diagnostics'. AGARDograph No. 296 section 2 (1988)
- 5 Kodak publication number F-26 (H). September (1987)
- 6 Bryanston-Cross, P.J., Epstein, A. 'The application of sub-micron particle visualisation for PIV at transonic speeds'. *Progress in Aerospace Science* 27 Pergamon Press (1990) 237-265
- 7 Bryanston-Cross, P.J., Towers, C.E., Harragama, S.P., Judge, T.R., Towers, D.P., Hopwood, S.T. 'The application of particle image velocimetry in a short duration transonic airfoil airfoil cascade'. ASME conference, Orlando, Florida, 3-6 June (1991)
- 8 Melling, A. 'Seedling gas flows for laser anemometry'. AGARD conference, 'Advanced Instrumentation for Aero Engine Components', Philadelphia, 19-23 May (1986) paper no 15
- 9 Hulst, H.C. *Laser Scattering By Small Particles*. Dover publications (1957)
- 10 Harris, A.E. 'Specification for study to identify laser holographic flow visualisation requirements for civil turboshaft powerplant installations'. Aircraft Research Association, internal report, February (1986)
- 11 Kompenhans, J., Reichman, J. 'Particle image velocimetry in a low turbulent wind tunnel and other flow facilities'. AGARD conference proceedings 'Advanced Instrumentation for Aero Engine Components', Philadelphia, 19-23 May (1986) paper no 35
- 12 Nichol, C. 'Preparation of polystyrene micro spheres for laser velocimetry in wind tunnels'. NASA Langley internal report
- 13 Seegmiller, H.L. 'Seeding subsonic, transonic and supersonic flows with 0.5 micron polystyrene spheres'. NASA Ames Research Centre, Moffett Field, California
- 14 Questar product information on QM1. Long Distance Microscope, Questar Corporation, PO Box 59, New Hope, PA 18938, USA
- 15 Babinet, M. *Diffraction*. Pergamon Press, series on *Topics in Optics* (1966)
- 16 Born, M., Wolf, E. *Principles of Optics*. Pergamon Press (1959)
- 17 Infinity K2 Long Distance Microscope product information. Infinity Photo-Optical Company, 706 Mohawk Drive, Suite 15, Boulder, CO 80303, USA
- 18 Manufacturer's specification for COHU model 4710 black and white CCD camera. CoHU, San Diego, California, USA
- 19 Manufacturer's specification for Pulnix model TM526 monochrome CCD camera. Pulnix Europe Ltd, Kapa Complex, Wade Road, Basingstoke, Hants RG24 OPL, UK
- 20 Towers, C.E., Towers, D.P., Judge, T.R., Bryanston-Cross, P.J. 'A laser light sheet investigation into transonic external aerodynamics'. SPIE Proc Vol 1358, paper 192. High Speed Photography and Photonics. Churchill College, Cambridge, September, 1990
- 21 Judge, T.R., PhD thesis. Warwick University, November (1991)